Atmospheric Environment 123 (2015) 210–219

Contents lists available at ScienceDirect

Atmospheric Environment

journal homepage: www.elsevier.com/locate/atmosenv

Source and transportation of summer dust over the Tibetan Plateau

Rui Jia, Yuzhi Liu*, Bin Chen, Zhijuan Zhang, Jianping Huang

Key Laboratory for Semi-Arid Climate Change of the Ministry of Education, College of Atmospheric Sciences, Lanzhou University, Lanzhou, 730000, China

HIGHLIGHTS

- The Tibetan Plateau is subject to heavy loading of dusts during summer.
- Cold advection or front and low-pressure system contribute to the dust emission.
- Meteorological conditions and the topography benefit dust transport to the TP.
- The 'elevated heat pump' help transport dust vertically over the TP.

ARTICLE INFO

Article history:
Received 27 June 2015
Received in revised form
10 October 2015
Accepted 13 October 2015
Available online 19 October 2015

Keywords:
Tibetan plateau
Summer dust
Source
Transportation

ABSTRACT

Satellite observational evidences (Cloud-Aerosol Lidar and Infrared Pathfinder Satellite Observations, CALIPSO) have presented that the Tibetan Plateau (TP) is subject to heavy loading of dust aerosols during summer. Combining back trajectory and weather system analyses, the source and transportation of summer Tibetan dust from 2007 to 2014 were investigated. The Tibetan dust is mainly from the Taklimakan Desert and partially from the Gurbantunggut Desert and Great Indian Thar Desert. Case study indicates that the meteorological conditions together with the topography benefit the dust emission adjacent to the TP and the transport toward the plateau. When a cold advection or front developed by strong cold advection passes, dust particles are emitted into the atmosphere from the Taklimakan and Gurbantunggut deserts and then transported to the northern slope of the TP with northeasterly wind induced by the Altai and Tian Shan mountains. For the period from 2007 to 2014, the correlation coefficient of the monthly frequencies of summer dust events over the TP and cold advection passing the Taklimakan and Gurbantunggut deserts were as high as 0.68 and 0.34, respectively. Differently, although the correlation is limited, much TP dust mobilized from the Great Indian Thar Desert is associated with the passing low-pressure system activity and generally polluted by anthropogenic aerosols. The polluted dust is further transported to the southern slope of the TP by the prevailing westerly wind. Investigations on the source and transportation of summer dust over the TP provide a solid foundation of data that can be used to reveal the role of TP dust in the radiation balance, hydrological cycle, and monsoon cycle in India and East Asia.

1. Introduction

Aerosols consist of solid and liquid particles are suspended in the atmosphere and can remain suspended for several days. Aerosols play a crucial role in the radiation balance of the earth-atmosphere system as well as global climate change (Han et al., 2013; Huang et al., 2014; Liu et al., 2011, 2013a, 2014b). Aerosols have significant effects on the radiation balance by scattering and absorbing radiation energy (direct effect) (Ju and Han, 2011; Zhang et al., 2009) or altering cloud microphysical properties (indirect and semi-direct effect) (Huang et al., 2006a, b; 2010; Sakaeda et al., 2011; Zhang et al., 2015; Rosenfeld et al., 2008). As an important component of absorbing aerosols, dust aerosols spread widely over a continent, heat the atmosphere by absorbing solar and emitting thermal radiation and lead to air pollution (Huang et al., 2009, 2011; Shao et al., 2011; Wang et al., 2013). Dust aerosols emitted from Asian deserts have a harmful influence on human health and can travel across the Pacific along the jet stream to the North American continent (Alizadeh-Choobari et al., 2014; Huang et al., 2008; Uno et al., 2001; Liu et al., 2013b). The transported dust aerosols may also modulate marine biogeochemical processes because of their high mineral component (Han et al., 2006).

* Corresponding author.
E-mail address: liuyzh@lzu.edu.cn (Y. Liu).

http://dx.doi.org/10.1016/j.atmosenv.2015.10.038
1352-2310/

Most of the studies on Asian dust have focused on the period of late winter or spring (Chen et al., 2009; Han et al., 2006; Liu et al., 2011; Uno et al., 2001; Sun et al., 2001; Wang et al., 2005). The observations from recently launched CALIPSO satellite show that dust events occur over the Taklimakan throughout the whole year and dust aerosols may even accumulate over the northern slope of the Tibetan Plateau (TP) (Huang et al., 2007; Liu et al., 2008b). However, there are very few studies analyzing the dust storm except for late winter and springs systematically and comprehensively. Chen et al. (2013, 2014b) further indicate that the main components of aerosols transported to the TP are dust aerosols, and the transported dusts reach a peak in summer. The TP is the tallest and most complex plateau on the Earth, and it has a great influence on the atmospheric circulation, hydrologic cycles, and regional and global climate change (Zhou et al., 2013a; Liu et al., 2007; Wu et al., 2006). It provides an elevated heat source to the middle-troposphere in summer (Yang et al., 2009; Wonsick et al., 2014). The TP is located at the convergence of several important natural and anthropogenic aerosol sources and the vertical flow induced by the heat source, i.e., the 'elevated heat pump' effect, could trigger strong convergence and assist in the vertical transport of dust aerosols from neighboring sources (Lau et al., 2006; Yang et al., 1992).

Once the dust aerosols are transported to the TP, they may affect the thermal structure of the atmosphere, surface albedo, and radiative balance and eventually modify the hydrological cycle and monsoon cycle in India and East Asia (Huang et al., 2009; Kuhlmann and Quaas, 2010; Qian et al., 2011; Lau et al., 2010). Although a number of studies have investigated dust aerosols over the TP (Huang et al., 2007; Liu et al., 2008a; Chen et al., 2013) as well as the drivers of dust storms (Heinold et al., 2013; Hopsch et al., 2007; Karam et al., 2009, 2010; Kumar et al., 2014), the meteorological mechanisms behind the mobilization and transportation of summer dust over the TP should be further studied.

Summer (June to August) dust aerosols over the TP were investigated in this study. Based on the CALIPSO data, we were able to detect intense dust events that occur in summer for the period 2007–2014. The spatial distribution of dust particle sizes, irregularity and intensity of a typical dust event that occurred on 15 June 2009 were analyzed via CALIPSO data. Combining the Hybrid Single Particle Lagrangian Integrated Trajectory (HYSPLIT) model, meteorological conditions derived from the European Center for Medium-Range Weather Forecasts (ECMWF) ERA-Interim reanalysis dataset and red-green-blue (RGB) color composite cloud images from MODIS (Moderate Resolution Imaging Spectroradiometer), the processes of dust emission and transportation were comprehensively investigated. Finally, a statistical analysis of the summer dust events over the TP and weather systems over the dust sources from 2007 to 2014 was conducted.

2. Dataset and methods

2.1. Dataset

Profiles of the total attenuated backscatter at 532 and 1064 nm, depolarization ratio at 532 nm and color ratio from CALIPSO Level 1B data combined with aerosol optical depth (AOD) from Level 2 Aerosol Layer data are used to detect dust aerosols and explore their vertical distribution. The distributions of cloud and aerosol from CALIPSO Lidar Vertical Feature Mask (VFM) product are also analyzed. The ECMWF ERA-Interim dataset is used to explore the emission and transportation mechanism of dust aerosols from a meteorological perspective.

The vertical and horizontal resolution of the CALIPSO data varies as a function of altitude. Because aerosols and clouds generally have larger spatial variabilities and stronger backscatter intensities at lower altitudes, this study focuses on heights ranging from 0 to 10 km above sea level (ASL), which have greater resolutions. For altitudes ranging from −0.5–8.2 km, the downlinked-sampling resolution is 30 m vertically and 1/3 km horizontally for 532 nm data, whereas the resolution is 60 m vertically and 1/3 km horizontally for 1064 nm data. For altitudes at 8.2–20.2 km, the vertical and horizontal resolutions are 60 m and 1 km for both 532 nm and 1064 nm data. The Level 2 layer product provides information on a horizontal grid of 5 km along the satellite orbit. Feature classifications from the VFM data are stored as a sequence of 5515 element arrays with the same resolution as the Level 1B 532 nm data.

To investigate the emission and transportation mechanisms of dust toward the TP, daily meteorological contours of U, V component of wind speed, vertical velocity, geopotential height and temperature from the ECMWF ERA-Interim reanalysis dataset are analyzed. The reanalysis data used in this study have a $1.0^\circ \times 1.0^\circ$ latitude/longitude spatial resolution and 37 pressure levels in the vertical direction with a temporal resolution of 6 h (at 00, 06, 12 and 18 UTC).

To understand the TP dust storm more systematically, AOD distribution from CALIPSO Level 3 and MISR (Multi-angle Imaging Spectroradiometer) Level 3 are also analyzed. CALIPSO and MISR data are retrieved from multiple orbits at a monthly time scale on geographic grids of $2^\circ \times 5^\circ$ and $0.5^\circ \times 0.5^\circ$ (latitude/longitude), respectively. The observation of MISR can even retrieve aerosol properties over highly reflective surfaces, such as deserts, with a high spatial sampling resolution of 275×1100 m.

2.2. Methods

The total attenuated backscatter coefficient at 532 nm, depolarization ratio and AOD from CALIPSO are combined to identify dust aerosols. The total attenuated backscatter coefficient at 532 nm, which reflects the intensity of particle backscatter extinction, can be used to separate aerosols from clouds because the backscatter signal from clouds is much larger (Huang et al., 2007, 2009; Zhou et al., 2013b; Winker et al., 2009). However, it may misclassify dense dust layers as clouds because of similar backscattering intensities (Huang et al., 2009; Liu et al., 2014a, 2008b). The depolarization ratio, defined as ratio of perpendicular to parallel components of the attenuated backscatter at 532 nm, can indicate the irregularity of particles in the atmosphere, with larger depolarization ratios indicating more irregular in shape. Because of the nonsphericity, dust aerosol has a larger depolarization ratio than water cloud and other aerosol, and smaller value relative to ice cloud (Chen et al., 2014a; Liu et al., 2008a; Li et al., 2013). To identify dust aerosols in this study, thresholds of 0.0008–0.048 $km^{-1}sr^{-1}$ and 0.06–0.4 are selected for the total attenuated backscatter and depolarization ratios, respectively (Chen et al., 2009; Liu et al., 2008a; Li et al., 2013; Zhao et al., 2009). Simultaneously, the AOD is used to enhance the reliability of dust detection. Compared with the particle depolarization ratio, the volume depolarization ratio has a more straightforward calculation process. In this study, the volume depolarization ratio is used instead because it can identify dust aerosols and avoid potential errors in particulate retrieval (Liu et al., 2008a). By combining the total attenuated backscatter, volume depolarization ratio and AOD, dust aerosols can be distinguished from clouds and other aerosols.

The color ratio, defined as the ratio of 1064 nm and 532 nm attenuated backscatter, is used to describe particle sizes, and larger ratios correspond to larger particles. The vertical and horizontal distributions of aerosol types and/or clouds are analyzed by using the VFM product.

The HYSPLIT-4 model (fourth-generation of HYSPLIT model) combined with meteorological contours from the ECMWF ERA-

Interim are used to investigate the dust outbreak and transportation mechanism. The HYSPLIT transport model, which is provided by NOAA Air Resources Laboratory, is used to calculate simple air-parcel trajectories with interpolated meteorological fields. The meteorological data for the model have to be processed to a HYSPLIT compatible format. The 6-h-interval final archive data are generated from the NCEP (National Centers for Environmental Prediction) Global Data Assimilation System (GDAS) reanalysis 3-dimensional meteorological fields.

In this study, four-day back trajectories are calculated to investigate the most likely transportation pathways of the detected dust aerosols. The TP is a key region of land–atmosphere interactions, as it provides an elevated heat source to the middle-troposphere which could induce vertical updrafts, the 'elevated heat pump' effect (Yang et al., 2009; Wonsick et al., 2014). To obtain additional details on the emissions and transportation mechanism of dust over the TP and reveal the role of the 'elevated heat pump', a synthesis of synoptic conditions from reanalysis data and HYSPLIT-4 back trajectories is performed. The atmospheric circulation field at 500 hPa over East Asia is determined according to daily meteorological contours, which include the U, V components of wind, vertical velocity, geopotential height, and temperature from the ECMWF ERA-Interim. To substantiate the synoptic systems accurately, analysis of MODIS/Terra RGB color composite cloud images is also carried out. In addition, the back trajectory and 850 hPa meteorological field analyses are combined to discuss the transportation.

3. Results

As shown in Fig. 1, the TP extends over a latitude–longitude region of 25–40°N, 74–104°E and has an average elevation of 4500 m ASL (shown in the crimson box). Because of its particular orography and location, the TP plays a significant role in the generation of atmospheric circulation and circulation patterns through dynamic and thermal processes. According to its climatic characteristics (Jiang and Wang, 2000), the TP is divided into three parts (separated by the crimson dotted lines): the Northeast Region (area A: 33–40°N, 85–105°E), Western Region (area B: 25–40°N, 70–85°E) and the Southeast Region (area C: 25–40°N; 70–85°E). The thick dark-gray line indicates the orbit path of the CALIPSO over the TP on 15 June 2009.

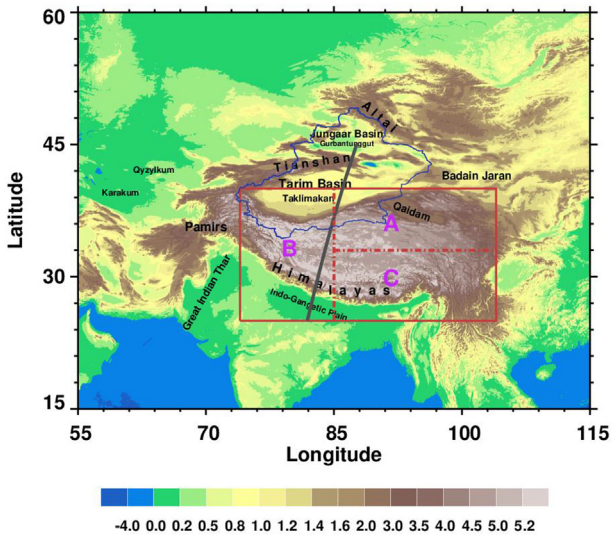

Fig. 1. Spatial topographical (km) distribution over the TP.

For the Northeast Region, the surrounding Taklimakan, Gurbantunggut and Badain Jaran deserts are the main dust sources, and a local desert in the Qaidam Basin also acts as a dust provider. The Western Region is surrounded by the Himalayas and Kunlun mountains as well as the Pamir Plateau and neighbors the Taklimakan Desert, Great Indian Thar Desert and deserts in the Central Asian. Compared with regions A and B, the Southeast Region is far from potential dust sources and the widespread rivers decrease the local dust emission.

3.1. Dust identification

In this section, the CALIPSO data are analyzed to identify dust aerosols over the TP, and a heavy dust event is investigated in detail. Fig. 2 presents the dust case measured by CALIOP on 15 June 2009 along the satellite orbit path (as shown in Fig. 1). The gray section in Fig. 2 indicates the topography. Generally, CALIPSO products indicate aerosols with a green-yellow-orange color scheme and clouds with white–gray. As shown in Figs. 2b and 2c, the total attenuated backscatter and volume depolarization ratio range from 0.002 to 0.005 $km^{-1}sr^{-1}$ and 0.06 to 0.3, respectively, which indicate that dust particles are the main components over the TP. Additionally, the white parts of Fig. 2b are considered as clouds and the deep-blue sections indicate that no signals were received because the laser cannot penetrate the clouds. The values of total attenuated backscatter indicate that the dust plumes are dense and spatially non-uniform, and the dust plumes over the northern slope are much denser than those over the southern slope. And the detection result agrees with the AOD (Fig. 2a). As suggested in Fig. 2d, obvious dense dust plumes (shown as orange dots) occur over both the southern and northern slopes of the TP and the dust plumes could extend upward to approximately 3–5 km ASL over the northern slope of the TP and to 5 km over the southern slope.

Fig. 3 presents orbit-altitude cross sections of the color ratio and feature classifications for the dust case. Fig. 3a shows that the color ratio over the northern TP slope ranges from 0.5 to 0.9 and remains relatively unchanged vertically, whereas it ranges from 0.5 to 1.2 and decreases with increasing altitude over the southern slope. The values show that the particle sizes don't vary with altitude over the

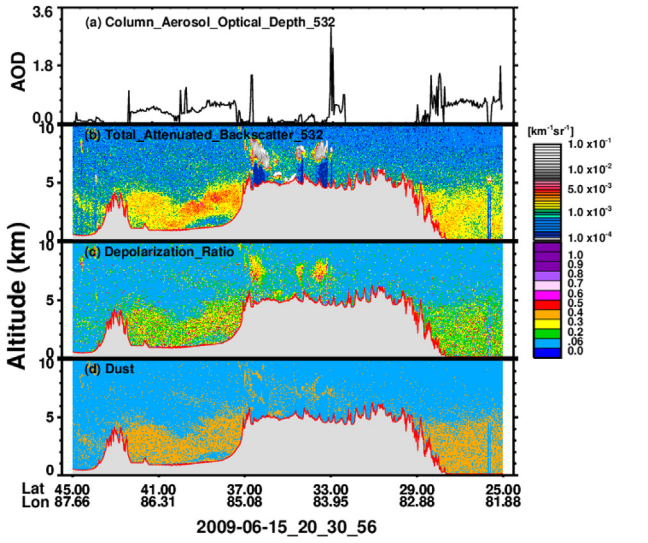

Fig. 2. Aerosol optical depth at 532 nm of the entire air column (a), altitude-orbit cross-sections of the total attenuated backscattering coefficient at 532 nm (b), depolarization ratio (c) and the detected dust particles (d) on 15 June 2009 along the CALIPSO orbit path.

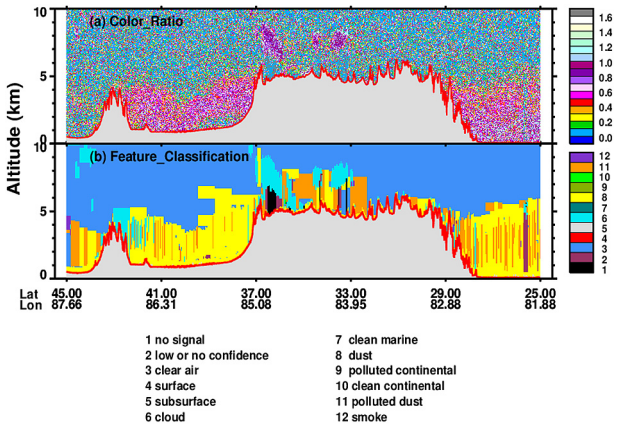

Fig. 3. The altitude-orbit cross-section of the color ratio (a) and classified particles (b) on 15 June 2009 along the CALIPSO orbit path.

northern slope but decrease with increasing altitude over the southern slope. Fig. 3b describes the spatial distribution of cloud and aerosol types, and thick dust plumes are observed over both the northern and southern slopes of the TP. Compared with the relatively pure dust over the northern slope, the dust over the southern slope is polluted by anthropogenic aerosols. Polluted dust particles even can be found above the TP, and they have polluted the clouds to some degree. As an important component of absorbing aerosols, the dust coupled with anthropogenic aerosols could provide an elevated heat source to the air (Lau et al., 2006).

3.2. Dust source analysis

Based on the identification of dust aerosols above, four-day-back-trajectory simulations produced with the HYSPLIT-4 model have been used to explore the most likely sources and transportation routes of these TP dusts. The back-trajectory simulations

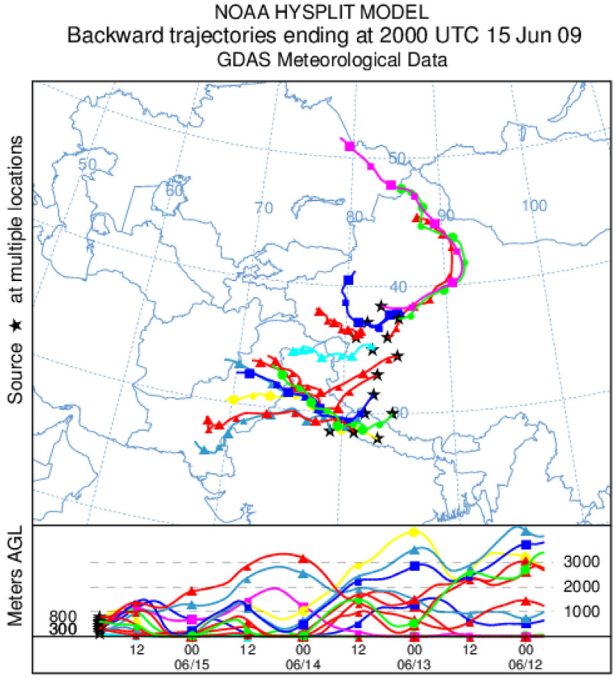

Fig. 4. Four-day back trajectories of air parcels climbing up the TP on 15 June 2009.

are shown in Fig. 4, and the dust-trajectory starting locations, which have been determined through CALIPSO observations, are marked with black stars. The trajectories are marked with different colors for starting points with different altitudes, and the altitudes of the air-entrained dust particles during transportation are provided at the bottom of Fig. 4. The dust aerosols over the TP primarily originate from the neighboring Taklamakan Desert, Great Indian Thar Desert, Indo-Gangetic Plain and Gurbantunggut Desert. Over the southern TP slope, the dust particles primarily originate from the Great Indian Thar Desert and the Indo-Gangetic Plain; however, the dust particles over the northern slope mainly originate from the Taklamakan and Gurbantunggut deserts. Combining with Fig. 3b, it suggests that the aerosols over the TP and the southern TP slope may be the dust, originating from the Great Indian Thar Desert, polluted by anthropogenic emissions from the Indo-Gangetic Plain during the transport.

As indicated in a number of studies (Aoki et al., 2005; Knippertz and Todd, 2012; Park et al., 2013; Yang et al., 2012), dust emissions are highly dependent on synoptic features, and their transportation is principally driven by the general atmospheric circulation. To investigate the dynamic mechanisms behind, the meteorological contours at 12:00 UTC (Figs. 5–7) combined with MODIS/Terra RGB color composite cloud images (Fig. 8) on 12–15 June 2009 in the vicinity of the TP are further investigated. Fig. 5 shows the spatial distributions of 500-hPa geopotential height (contours) and temperature (colors). Figs. 6 and 7 present the vector fields of horizontal winds (thin black arrows) and distribution of vertical velocities (colors, blue for downdrafts and red for updrafts) at 500 hPa and 850 hPa. Obvious vertical updrafts could be found in Figs. 6 and 7 over the TP and its neighborhood. A deep low-pressure system (East Asia Trough) with strong winds and cold air covers the area from Western Siberia to the northwest border of China on 12 June (Figs. 5a and 6a). Northwesterly winds behind the East Asia Trough bypass the Tian Shan Mountains and bring a large amount of cold air into the Tarim Basin. As shown in Fig. 5b, the cold low-pressure system develops more deeply and moves slightly to the east on 13 June. A strong temperature gradient occurs in northern Xinjiang (a province of China, as the blue curve shows in Fig. 1) because of the cold advection behind the East Asia Trough. The collision of incoming cold air and warm updrafts from the heat surface of the Taklimakan Desert leads to the formation of a cold front at the northwest border of China, which also can be found in the remote sensing cloud images (as the thick line shown in Fig. 8a). It is beneficial to dust emissions due to the dry warm air before the cold front associated with the updrafts over the bare soil. Cold air is also brought to the Junggar Basin on 13 June, and similar conditions are observed over the Gurbantunggut Desert (Figs. 5b, 6b and 8b). With the eastward movement of the cold front crossing Tian shan and Altai mountains to the basins, the downdrafts caused by topography lead the cold front to be weaken, which is the main reason of indistinct cold front but thin cloud shown in cloud images (Figs. 8b and 8c). Also, as shown in Figs. 5c and 6c, the low-pressure system begins to weaken on 14 June 2009, and significant updrafts over the Taklimakan and Gurbantunggut deserts weaken and even turn to downdrafts, which could reduce the dust emissions. The cold low-pressure system system moves eastward further on 15 June 2009 (Fig. 8d), and the synoptic airflow in the East Asia changes from meridional to zonal, which reduces the cold air brought to the Tarim and Junggar basins as shown in Figs. 5c and 5d.

As shown in Fig. 4, the dust particles and climb along the topography during the transportation process. Fig. 7 shows the vertical velocities and wind vectors at 850 hPa at 12:00 UTC on 12–15 June. The winds near the surface are easily affected by the topography. The Tian Shan and Altai mountains block the strong

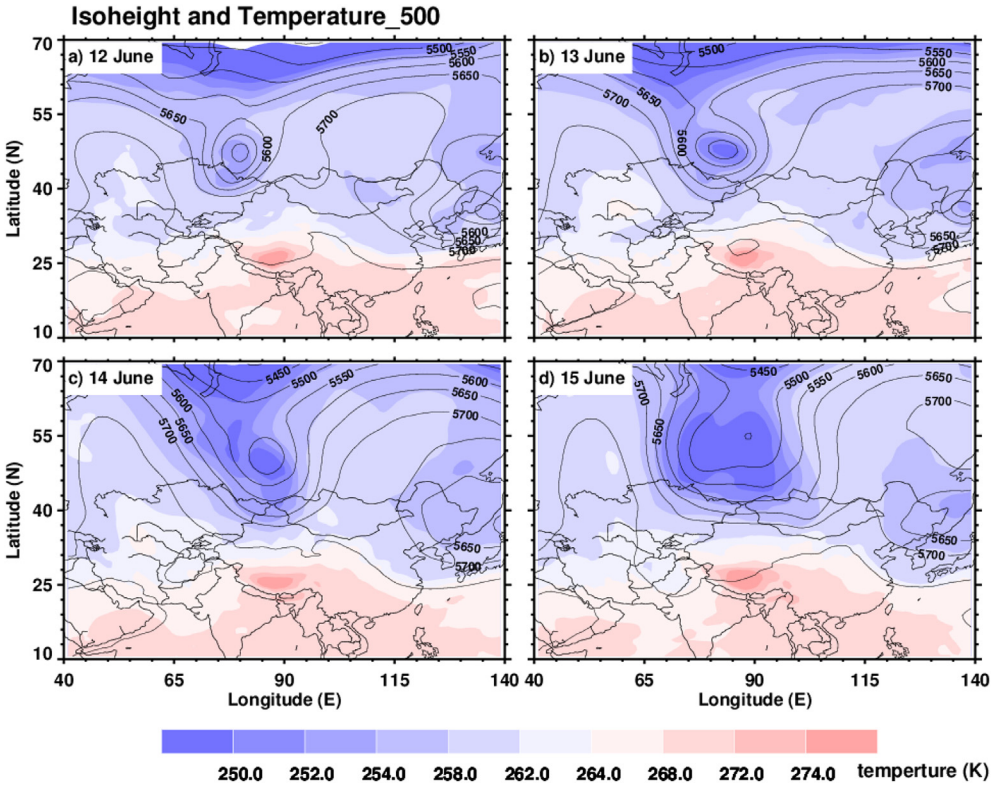

Fig. 5. Spatial distribution of geopotential height (black contour) and temperature (color) at 500 hPa from ERA-Interim at 12:00 UTC for the period from 12 to 15 June 2009. (For interpretation of the references to colour in this figure legend, the reader is referred to the web version of this article.)

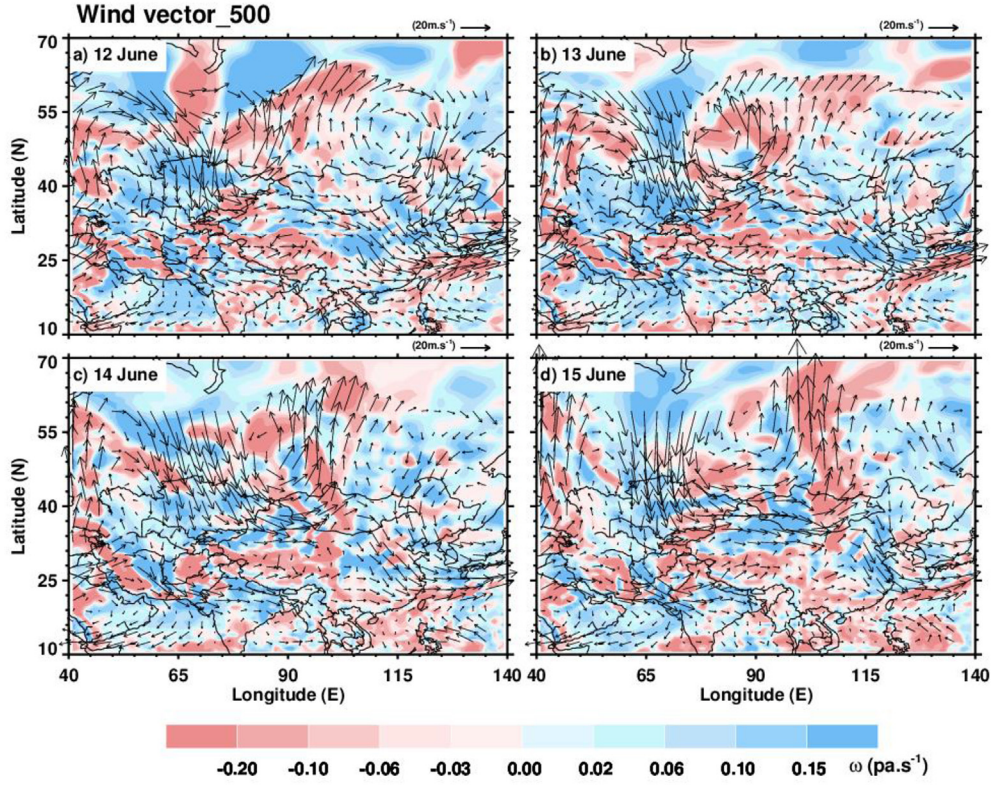

Fig. 6. Spatial distribution of the wind vector (arrows) and vertical velocity (colors, blue for downdrafts and red for updrafts) at 500 hPa from ERA-Interim at 12:00 UTC for the period from 12 to 15 June 2009.

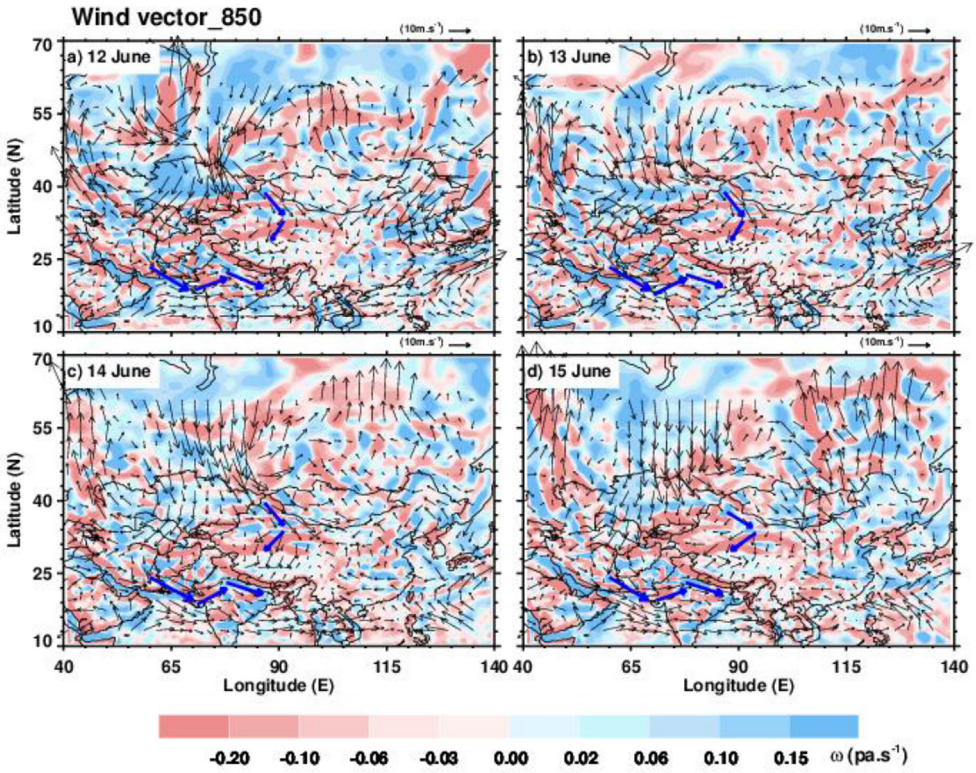

Fig. 7. Same as in Fig. 6 but for 850 hPa.

northwesterly winds and lead to the accumulation of air along the corridor, and the airflow then turns southward and conforms to the topography. Such conditions induce the northwesterly winds traveling along the corridor to turn northeasterly around the southeastern side of the Tian Shan Mountains, which is indicated by blue arrows in Fig. 7. The dust particles entrained into the air current are forced toward the TP, by passing the Altai and Tian Shan mountains. The transported dust particles stack up over the north slope of the TP and are brought up to the plateau as they are driven by the updrafts, i.e., the 'elevated heat pump' effect (Yang et al., 1992).

Unlike the conditions over the Taklamakan and Gurbantunggut deserts, profound updrafts and strong winds persist over the Great Indian Thar Desert (Figs. 6 and 7). Concurrently, an inconspicuous low-pressure system (cyclone system) appears and develops during 14–15 June 2009 (Figs. 6c and 6d), which presents counterclockwise thick cloud in the cloud image (as the rectangle shown in Fig. 8d). These meteorological conditions help transport dust emitted from the Great Indian Thar Desert. The TP and Pamir Plateau induce the prevailing westerlies along the plateaus (as the blue arrows shown in Fig. 7). Further more, combining with Fig. 4, the winds may bring dust aerosols to the TP, and the particles may be brought up to the southern slope of the TP by the updrafts. Combining with Fig. 3b, it suggests that the aerosols over the TP and the southern TP slope may be the dust, originating from the Great Indian Thar Desert, polluted by anthropogenic emissions from the Indo-Gangetic Plain during the transport.

Overall, the studied dust event occurs during a changing period of atmospheric circulation in East Asia. The simulated results from the HYSPLIT-4 model show that dust aerosols over the northern slope of the TP mainly originate from the Taklamakan and Gurbantunggut deserts. The dust emissions over these two deserts are generated by a mesoscale cold-front system. The meteorological conditions and terrain provide favorable conditions for the propagation of airstream-entrained dust particles across the eastern side of the Tian Shan Mountains toward the TP. The transported dust particles stack up at the northern slope of the TP and even climb to surpass the TP, which is consistent with previous results (Chen et al., 2013; Huang et al., 2007). The Great Indian Thar Desert is the source of dust aerosols over the southern slope of the TP, and the dust could be triggered by the profound updrafts and strong winds and transported to the TP by the prevailing winds. The results based on meteorological conditions analysis are consistent with the HYSPLIT-4 model simulations. The 'elevated heat pump' effect is beneficial to the transport of dust and anthropogenic aerosols to the TP. Further more, the dust coupled with anthropogenic aerosols transported to the TP could heat up the elevated surface air through absorbing radiation energy which will reinforce the 'elevated heat pump' effect in turn (Lau et al., 2006).

3.3. Statistical analysis

Statistical analyses have been conducted for summer dust events detected over three regions of the TP for the period 2007–2014, and simulations of back trajectories have been performed to statistically investigate the most likely dust sources and transport routes. The dust detections were conducted for each day in the summer during 2007–2014 using the method mentioned in Section 3.1. For each dust event detection, the thresholds of 0.0008–0.048 $km^{-1}sr^{-1}$ and 0.06–0.4 for the total attenuated backscatter and depolarization ratio were adopted and the simulations of back trajectories have been done.

The frequencies of summer TP dust events from 2007 to 2014 are listed in Table 1 (A/B, A denotes the frequencies of dust events and B is for the frequencies of total samples), which indicates these events occurred 225, 154, and 20 times over the Northeast, Western

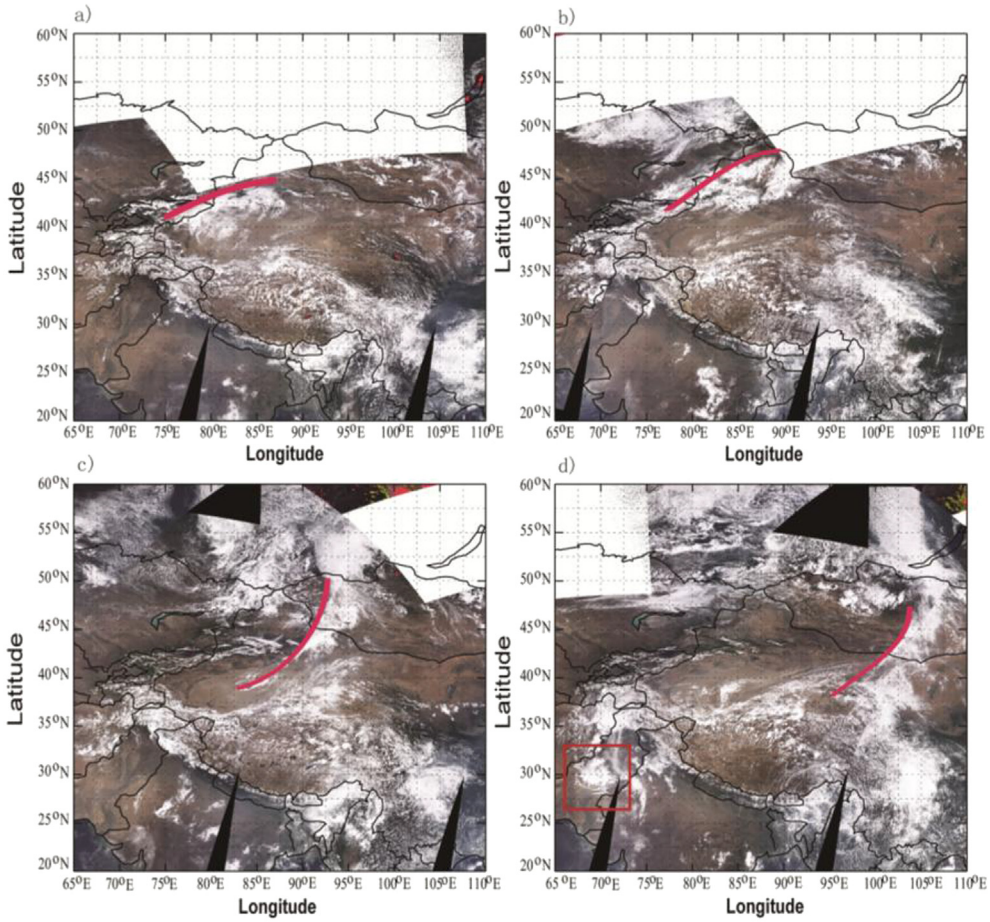

Fig. 8. RGB color composite cloud images observed from MODIS/Terra in the vicinity of the TP during 12–15 June 2009. (For interpretation of the references to colour in this figure legend, the reader is referred to the web version of this article.)

Table 1
Dust events in summer over the TP from 2007 to 2014 (frequency).

Region	Year								
	2007	2008	2009	2010	2011	2012	2013	2014	Total
A	30/90	24/80	33/89	30/88	21/76	20/79	32/90	35/87	225
B	22/66	22/60	25/66	12/62	19/55	14/57	18/64	22/65	154
C	0/90	3/80	5/88	2/87	0/76	4/81	4/90	2/84	20

and Southeast regions of the TP, respectively. To reveal the fact which of these regions is influenced most heavily by the dust storms, AOD distributions in the summer during 2007–2014 for above regions are compared (Fig. 9). Combining the dust event frequencies and AOD values, it can be concluded that the dust events primarily occur over the Northeast Region and the Western Region, and seldom occur over the Southeast Region.

Fig. 10 presents the frequencies of dust occurrence and corresponding sources based on the HYSPLIT-4 simulations for the detected cases listed in Table 1. For the Northeast Region, the main dust source is the Taklimakan Desert, which accounts for 65% of the detected dust events. The Gurbantunggut and Kumtag deserts both account for 32% of the dust events over the Northeast Region, and the Badain Jaran and Qaidam deserts both account for approximately 3% of the events. For the Western Region, the neighboring Taklimakan Desert and Great Indian Thar Desert account for 84% and 40% of the detected dust events, respectively. Because there may be two or more sources for a certain dust event, the sum of the percentages for a region is not equal to 100%. Dust events seldom occur over the Southeast Region, and the dust aerosols for these few cases mostly originate from the neighboring Taklimakan and Great Indian Thar deserts.

Based on the comprehensive analysis of the back trajectories and meteorological fields, the correlation between summer TP dust events and their potential contributing factors has been statistically investigated. As suggested in certain studies (Chen et al., 2013; Fiedler et al., 2014; Karam et al., 2009, 2010), cyclones (low-pressure system) and cold fronts are the predominant drivers of dust storms. However, it is difficult to quantify the dust density and low-pressure systems or cold front intensity from observational data. In this study, an alternative method was performed by investigating correlations among the frequencies between dust events and cold fronts/low-pressure systems.

Low-pressure systems rarely occur in the vicinity of the Gurbantunggut and Taklimakan deserts because of the especially long corridor and friction on the eastern side of the Tian Shan Mountains, whereas the northwesterly cold air and warm updrafts from the hot desert surface are favorable for the development of cold front/advection. Because of the topographic countercheck of the Pamir Plateau, cold air seldom migrates to the Great Indian Thar Desert, and friction on the western side of the plateau easily induces cyclonical-bending flow. Thus, correlations among the monthly frequencies of cold advections passing the Taklimakan Desert (Fig. 11a) and Gurbantunggut Desert (Fig. 11b), the low-pressure systems passing the Great Indian Thar Desert (Fig. 11c),

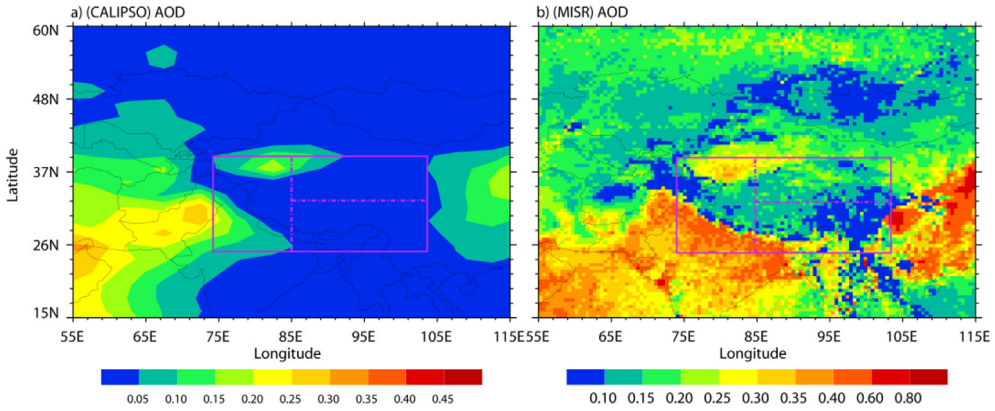

Fig. 9. AOD over the vicinity of the TP from CALIPSO (a) and MISR (b) of the summer during 2007–2014.

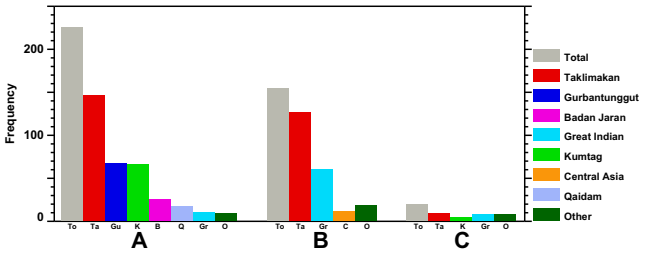

Fig. 10. Frequencies of summer dust events occurred over the three regions of the TP from 2007 to 2014. The gray bars represent the total frequencies of dust occurrences, and the colored bars represent the frequencies of dust sources. (For interpretation of the references to colour in this figure legend, the reader is referred to the web version of this article.)

and summer dust events over the TP for the period 2007–2014 are investigated. As shown in Fig. 11a, the correlation coefficient of the monthly frequencies between the summer TP dust events from 2007 to 2014 and cold advections passing the Taklimakan Desert is as high as 0.68. Although the Gurbantunggut and Great Indian Thar Deserts are not the main dust sources of the TP, fairly strong correlations are observed among the cold advections passing the Gurbantunggut Desert and low-pressure systems passing the Great Indian Thar Desert with TP dust events (0.34 and 0.29, respectively). In general, the dust aerosols are emitted from the Taklimakan and Gurbantunggut deserts as a result of passing cold-front systems and from the Great Indian Thar Desert due to low-pressure systems, and then these aerosols are transported to the TP by prevailing winds.

4. Conclusions and discussion

Changes of the synoptic airflow in the East Asia from meridional to zonal cause dust events over the TP to occur, and the dust particles primarily originate from the neighboring Taklamakan and Great Indian Thar Deserts and the Gurbantunggut Desert. The dust emissions from the Taklimakan and Gurbantunggut deserts, the dust sources of the northern TP slope, are initiated by the formation and development of a strong cold frontal system, whereas the emissions from Great Indian Thar Desert are induced by updrafts and strong winds associated with low-pressure systems. Geographical conditions induce the surrounding prevailing winds toward the TP. Because of the orography barrier, the Tian Shan and Altai mountains could produce an accumulation of air from the northwesterly winds and enable airflows along the corridor, which turn southwesterly toward the TP. Additionally, because of the topographic countercheck of the TP and Pamir Plateau, the prevailing westerlies flow along the plateaus. The meteorological conditions strongly affect the transportation, and the aerosols can even be lifted up and over the plateau by updrafts.

Case study and statistical analyses have shown that the dust aerosols primarily originate from the Taklimakan Desert. Additionally, the Gurbantunggut and Kumtag deserts and the local Qaidam Desert also provide abundant dust aerosols to the TP. Of the three regions investigated in this study, the Southeast Region, which is located at a significant distance from the dust sources, received a small amount of dust. However, the West Region receives dust aerosols that are emitted from the Great Indian Thar Desert and usually transported by the summer monsoon. For the Northeast Region, the dust aerosols from the Taklimakan, Gurbantunggut or Badan Jaran deserts are easily transported to or over

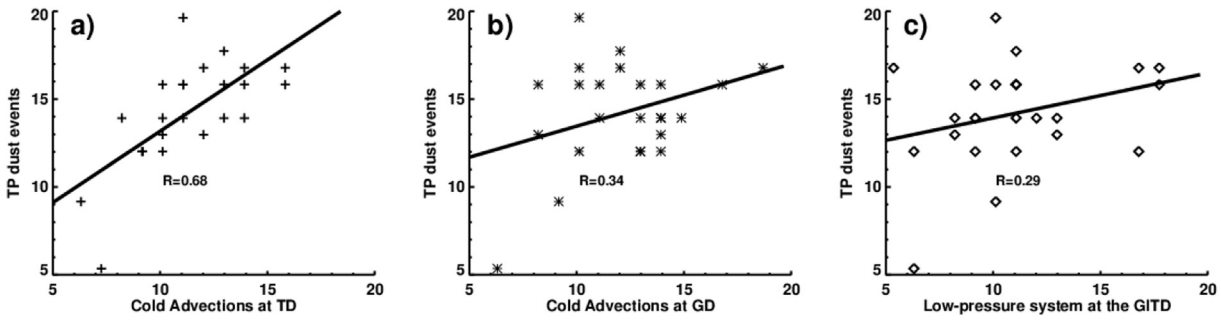

Fig. 11. Correlation of the monthly frequencies of summer dust events over the TP with (a) cold advections passing the Taklimakan Desert, (b) cold advections passing the Gurbantunggut Desert, and (c) cyclones passing the Great Indian Thar Desert from 2007 to 2014.

the TP.

The dust aerosols from the Taklimakan and Gurbantunggut deserts are emitted by passing cold advection, and those from the Great Indian Thar Desert are emitted by passing low-pressure systems. These aerosols are then transported to the TP with the prevailing winds and lifted up and over the plateau because of the 'elevated heat pump' effect. On the other hand, the absorption of solar radiation by dust aerosols coupled with anthropogenic aerosols over the slopes will heat up the elevated surface air and reinforce the 'elevated heat pump' effect in turn.

Although the satellite can observe and detect dust events over the TP, the spatial and temporal scanning limitations produce difficulties in understanding the distribution of dust aerosols over the TP. In future studies, a combination of satellite and model simulations should be performed to reveal the distribution, optical properties, and transportation of dust aerosols over the TP.

Acknowledgments

This research was jointly supported by the National Basic Research Program of China (2012CB955301), National Natural Science Foundation of China (41475095 and 41275006), Fundamental Research Funds for the Central Universities (lzujbky-2014-ct05, lzubjky-2014-109, and lzujbky-2009-k03), and China 111 project (B13045). The data for this paper are available at NASA Atmospheric Data Center (http://eosweb.larc.nasa.gov/) and ECMWF (http://data-portal.ecmwf.int/data/d/interim_daily/levtype=pl/). HYSPLIT model used in this paper is available at http://www.arl.noaa.gov/ready/hysplit4.html. The meteorological data corresponding to HYSPLIT compatible format is available in the public directory of ftp://gdas-server.iarc.uaf.edu/gdas1/.

References

Alizadeh-Choobari, O., Sturman, A., Zawar-Reza, P., 2014. A global satellite view of the seasonal distribution of mineral dust and its correlation with atmospheric circulation. Dynam. Atmos. Oceans 68, 20–34. http://dx.doi.org/10.1016/j.dynatmoce.2014.07.002.

Aoki, I., Kurosaki, Y., Osada, R., Sato, T., Kimura, F., 2005. Dust storms generated by mesoscale cold fronts in the Tarim Basin, Northwest China. Geophys. Res. Lett. 32 (6), L06807. http://dx.doi.org/10.1029/2004GL021776.

Chen, B., Zhang, P., Zhang, B., Jia, R., Zhang, Z., Wang, T., Zhou, T., 2014a. An overview of passive and active dust detection methods using satellite measurements. J. Meteor. Res. 28 (6), 1029–1040. http://dx.doi.org/10.1007/s13351-014-4032-4.

Chen, S., Huang, J., Zhao, C., Qian, Y., Leung, L.R., Yang, B., 2013. Modeling the transport and radiative forcing of Taklimakan dust over the Tibetan Plateau: a case study in the summer of 2006. J. Geophys. Res. Atmos. 118 (2), 797–812. http://dx.doi.org/10.1002/jgrd.50122.

Chen, S., Zhao, C., Qian, Y., Leung, L.R., Huang, J., Huang, Z., Bi, J., Zhang, W., Shi, J., Yang, L., Li, D., li, J., 2014b. Regional modeling of dust mass balance and radiative forcing over East Asia using WRF-Chem. Aeolian Res. 15, 15–30. http://dx.doi.org/10.1016/j.aeolia.2014.02.001.

Chen, Y., Mao, X., Huang, J., Zhang, H., Tang, Q., Pan, H., Wang, C., 2009. Vertical distribution characteristics of aerosol during a long-distance transport of heavy dust pollution. China Environ. Sci. 29 (05), 449–454.

Fiedler, S., Schepanski, K., Knippertz, P., Heinold, B., Tegen, I., 2014. How important are atmospheric depressions and mobile cyclones for emitting mineral dust aerosol in North Africa? Atmos. Chem. Phys. 14 (17), 8983–9000. http://dx.doi.org/10.5194/acp-14-8983-2014.

Han, Y., Fang, X., Xi, X., Song, L., Yang, S., 2006. Dust storm in Asia continent and its bio-environmental effects in the North Pacific: a case study of the strongest dust event in April, 2001 in central Asia. Chin. Sci. Bull. 51 (6), 723–730. http://dx.doi.org/10.1007/s11434-006-0723-2.

Han, Z., Li, J., Guo, W., Xiong, Z., Zhang, W., 2013. A study of dust radiative feedback on dust cycle and meteorology over East Asia by a coupled regional climate-chemistry-aerosol model. Atmos. Environ. 68, 54–63. http://dx.doi.org/10.1016/j.atmosenv.2012.11.032.

Heinold, B., Knippertz, P., Marsham, J.H., Fiedler, S., Dixon, N.S., Schepanski, K., Laurent, B., Tegen, I., 2013. The role of deep convection and nocturnal low-level jets for dust emission in summertime West Africa: estimates from convection-permitting simulations. J. Geophys. Res. Atmos. 118 (10), 4385–4400. http://dx.doi.org/10.1002/jgrd.50402.

Hopsch, S.B., Thorncroft, C.D., Hodges, K., Aiyyer, A., 2007. West African storm tracks and their relationship to Atlantic tropical cyclones. J. Clim. 20 (11), 2468–2483. http://dx.doi.org/10.1175/JCLI4139.1.

Huang, J., Bing, L., Minnis, P., Wang, T., Wang, X., Hu, Y., Yi, Y., Ayers, J.K., 2006a. Satellite-based assessment of possible dust aerosols semi-direct effect on cloud water path over East Asia. Geophys. Res. Lett. 33 (19), L19802. http://dx.doi.org/10.1029/2006gl026561.

Huang, J., Fu, Q., Su, J., Tang, Q., Minnis, P., Hu, Y., Yi, Y., Zhao, Q., 2009. Taklimakan dust aerosol radiative heating derived from CALIPSO observations using the Fu-Liou radiation model with CERES constraints. Atmos. Chem. Phys. 9 (12), 4011–4021. http://dx.doi.org/10.5194/acp-9-4011-2009.

Huang, J., Fu, Q., Zhang, W., Wang, X., Zhang, R., Ye, H., Warren, S.G., 2011. Dust and black carbon in seasonal snow across northern china. B. Am. Meteorol. Soc. 92 (2), 175–181. http://dx.doi.org/10.1175/2010BAMS3064.1.

Huang, J., Minnis, P., Lin, B., Wang, T., Yi, Y., Hu, Y., Sunny, S.M., Ayers, K., 2006b. Possible influences of Asian dust aerosols on cloud properties and radiative forcing observed from MODIS and CERES. Geophys. Res. Lett. 33 (6), L06824. http://dx.doi.org/10.1029/2005GL024724.

Huang, J., Minnis, P., Yan, H., Yi, Y., Chen, B., Zhang, L., Ayers, J.K., 2010. Dust aerosol effect on semi-arid climate over Northwest China detected from A-Train satellite measurements. Atmos. Chem. Phys. 10 (14), 6863–6872. http://dx.doi.org/10.5194/acp-10-6863-2010.

Huang, J., Minnis, P., Chen, B., Huang, Z., Liu, Z., Zhao, Q., Yi, Y., Ayers, J.K., 2008. Long-range transport and vertical structure of Asian dust from CALIPSO and surface measurements during PACDEX. J. Geophys. Res. Atmos. 113 (D23), D23212. http://dx.doi.org/10.1029/2008JD010620.

Huang, J., Minnis, P., Yi, Y., Tang, Q., Wang, X., Hu, Y., Liu, Z., Ayers, K., Trepte, C., Winker, D., 2007. Summer dust aerosols detected from CALIPSO over the Tibetan Plateau. Geophys. Res. Lett. 34 (18), L18805. http://dx.doi.org/10.1029/2007gl029938.

Huang, J., Wang, T., Wang, W., Li, Z., Yan, H., 2014. Climate effects of dust aerosols over East Asian arid and semiarid regions. J. Geophys. Res. Atmos. 119 (19), 11398–11416. http://dx.doi.org/10.1002/2014JD021796.

Jiang, H., Wang, K., 2000. Analysis of the surface temperature on the Tibetan Plateau from satellite. Plateau Meteorol. 19 (3), 323–330.

Ju, L., Han, Z., 2011. Direct radiative forcing and climatic effects of aerosols over east asia by RegCM3. Atmos. Ocean. Sci. Lett. 4 (06), 363–367.

Karam, D.B., Flamant, C., Cuesta, J., Pelon, J., Williams, E., 2010. Dust emission and transport associated with a Saharan depression: February 2007 case. J. Geophys. Res. Atmos. 115 (D4), D00H27. http://dx.doi.org/10.1029/2009jd012390.

Karam, D.B., Flamant, C., Tulet, P., Todd, M.C., Pelon, J., Williams, E., 2009. Dry cyclogenesis and dust mobilization in the intertropical discontinuity of the West African Monsoon: a case study. J. Geophys. Res. Atmos. 114 (D5), D05115. http://dx.doi.org/10.1029/2008JD010952.

Knippertz, P., Todd, M.C., 2012. Mineral dust aerosols over the Sahara: meteorological controls on emission and transport and implications for modeling. Rev. Geophys. 50 (1), RG1007. http://dx.doi.org/10.1029/2011rg000362.

Kuhlmann, J., Quaas, J., 2010. How can aerosols affect the Asian summer monsoon? Assessment during three consecutive pre-monsoon seasons from CALIPSO satellite data. Atmos. Chem. Phys. 10, 4673–4688. http://dx.doi.org/10.5194/acp-10-4673-2010.

Kumar, R., Barth, M.C., Pfister, G.G., Naja, M., Brasseur, G.P., 2014. WRF-Chem simulations of a typical pre-monsoon dust storm in northern India: influences on aerosol optical properties and radiation budget. Atmos. Chem. Phys. 14, 2431–2446. http://dx.doi.org/10.5194/acp-14-2431-2014.

Lau, K.M., Kim, M.K., Kim, K.M., 2006. Asian summer monsoon anomalies induced by aerosol direct forcing: the role of the Tibetan Plateau. Clim. Dynam. 26, 855–864. http://dx.doi.org/10.1007/s00382-006-0114-z.

Lau, W.K.M., Kim, M.K., Kim, K.M., Lee, W.S., 2010. Enhanced surface warming and accelerated snow melt in the Himalayas and TibetanPlateau induced by absorbing aerosols. Environ. Res. Lett. 5 (2), 025204. http://dx.doi.org/10.1088/1748-9326/5/2/025204.

Li, H., Zheng, W., Gong, Q., 2013. An analysis on detection of a sand-dust weather over taklimakan desert based on polarization micro-pulse lidar. Desert Oasis Meteorol. 7 (1), 1–5.

Liu, D., Wang, Z., Liu, Z., Winker, D., Trepte, C., 2008a. A height resolved global view of dust aerosols from the first year CALIPSO lidar measurements. J. Geophys. Res. Atmos. 113 (D16), D16214. http://dx.doi.org/10.1029/2007JD009776.

Liu, J., Chen, B., Huang, J., 2014a. Discrimination and validation of clouds and dust aerosol layers over the Sahara desert with combined CALIOP and IIR measurements. J. Meteor. Res. 28 (2), 185–198. http://dx.doi.org/10.1007/s13351-014-3051-5.

Liu, Y., Bao, Q., Duan, A., Qian, Z., Wu, G., 2007. Recent progress in the impact of the Tibetan Plateau on climate in China. Adv. Atmos. Sci. 24 (6), 1060–1076. http://dx.doi.org/10.1007/s00376-007-1060-3.

Liu, Y., Huang, J., Shi, G., Takamura, T., Khatri, P., Bi, J., Shi, J., Wang, T., Wang, X., Zhang, B., 2011. Aerosol optical properties and radiative effect determined from sky-radiometer over Loess Plateau of Northwest China. Atmos. Chem. Phys. 11 (22), 11455–11463. http://dx.doi.org/10.5194/acp-11-11455-2011.

Liu, Y., Shi, G., Xie, Y., 2013a. Impact of dust aerosol on glacial-interglacial climate. Adv. Atmos. Sci. 30 (6), 1725–1731. http://dx.doi.org/10.1007/s00376-013-2289-7.

Liu, Y., Jia, R., Dai, T., Xie, Y., Shi, G., 2014b. A review of aerosol optical properties and radiative effects. J. Meteor. Res. 28 (6), 1003–1028. http://dx.doi.org/10.1007/s13351-014-4045-z.

Liu, Z., Liu, D., Huang, J., Vaughan, M., Uno, I., Sugimoto, N., Kittaka, C., Trepte, C., Wang, Z., Hostetler, C., Winker, D., 2008b. Airborne dust distributions over the

Tibetan Plateau and surrounding areas derived from the first year of CALIPSO lidar observations. Atmos. Chem. Phys. 8 (16), 5045–5060. http://dx.doi.org/10.5194/acp-8-5045-2008.

Liu, Z., Fairlie, T.D., Uno, I., Huang, J., Wu, D., Omar, A., Kar, J., Vaughan, M., Rogers, R., Winker, D., Trepte, C., Hu, Y., Sun, W., Lin, B., Cheng, A., 2013b. Transpacific transport and evolution of the optical properties of Asian dust. J. Quant. Spectrosc. RA 116, 24–33. http://dx.doi.org/10.1016/j.jqsrt.2012.11.011.

Park, S.-U., Choe, A., Park, M.-S., 2013. A simulation of asian dust events observed from 20 to 29 December 2009 in Korea by using ADAM2. Asia-Pacific J. Atmos. Sci. 49 (1), 95–109. http://dx.doi.org/10.1007/s13143-013-0011-4.

Qian, Y., Flanner, M.G., Leung, L.R., Wang, W., 2011. Sensitivity studies on the impacts of Tibetan Plateau snowpack pollution on the Asian hydrological cycle and monsoon climate. Atmos. Chem. Phys. 11 (5), 1929–1948. http://dx.doi.org/10.5194/acp-11-1929-2011.

Rosenfeld, D., Lohmann, U., Raga, G.B., O'Dowd, C.D., Kulmala, M., Fuzzi, S., Reissell, A., Andreae, M.O., 2008. Flood or drought: how do aerosols affect precipitation? Science 321 (5894), 1309–1313. http://dx.doi.org/10.1126/science.1160606.

Sakaeda, N., Wood, R., Rasch, P.J., 2011. Direct and semidirect aerosol effects of southern African biomass burning aerosol. J. Geophys. Res. Atmos. 116 (D12), D12205. http://dx.doi.org/10.1029/2010jd015540.

Shao, Y., Wyrwoll, K.H., Chappell, A., Huang, J., Lin, Z., McTainsh, G.H., Mikami, M., Tanaka, T.Y., Wang, X., Yoon, S., 2011. Dust cycle: an emerging core theme in earth system science. Aeolian Res. 2 (4), 181–204. http://dx.doi.org/10.1016/j.aeolia.2011.02.001.

Sun, J., Zhang, M., Liu, T., 2001. Spatial and temporal characteristics of dust storms in China and its surrounding regions, 1960–1999: relations to source area and climate. J. Geophys. Res. 106, 10325–10333.

Uno, I., Amano, H., Emori, S., Kinoshita, K., Matsui, I., Sugimoto, N., 2001. Trans-Pacific yellow sand transport observed in April 1998: a numerical simulation. J. Geophys. Res. Atmos. 106 (D16), 18331–18344. http://dx.doi.org/10.1029/2000jd900748.

Wang, H., Shi, G., Zhu, J., Chen, B., Che, H., Zhao, T., 2013. Case study of longwave contribution to dust radiative effects over East Asia. Chin. Sci. Bull. 58 (30), 3673–3681. http://dx.doi.org/10.1007/s11434-013-5752-z.

Wang, S., Wang, J., Zhou, Z., Shang, K., 2005. Regional characteristics of three kinds of dust storm events in China. Atmos. Environ. 39, 509–520.

Winker, D.M., Vaughan, M.A., Omar, A., Hu, Y., Powell, K.A., Liu, Z., Hunt, W.H., Young, S.A., 2009. Overview of the CALIPSO Mission and CALIOP data processing Algorithms. J. Atmos. Ocean. Tech 26 (11), 2310–2323. http://dx.doi.org/10.1175/2009jtecha1281.1.

Wonsick, M.M., Pinker, R.T., Ma, Y., 2014. Investigation of the “elevated heat pump” hypothesis of the Asian monsoon using satellite observations. Atmos. Chem. Phys. 14, 8749–8761. http://dx.doi.org/10.5194/acp-14-8749-2014.

Wu, G., Mao, J., Duan, A., Zhang, Q., 2006. Current progresses in study of impacts of the Tibetan Plateau on Asian summer climate. Acta Meteorol. Sin. 02, 144–158.

Yang, K., Chen, Y.-Y., Qin, J., 2009. Some practical notes on the land surface modeling in the Tibetan Plateau. Hydrol. Earth Syst. Sci. 13, 687–701. http://dx.doi.org/10.5194/hess-13-687-2009.

Yang, W., Ye, D., Wu, G., 1992. The influence of the Tibetan Plateau on the thermal and circulation fields over East Asia in summer II: main features of the local circulation fields and the large-scale vertical circulation fields. Sci. Atmos. Sinica 16 (03), 287–301.

Yang, X., He, Q., Ali, M., Huo, W., Liu, X., Strake, M., 2012. A field experiment on dust emission by wind erosion in the taklimakan desert. Acta Meteorol. Sin. 26 (02), 241–249. http://dx.doi.org/10.1007/s1335-1012-0209-x.

Zhang, D., Liu, D., Luo, T., Wang, Z., Yin, Y., 2015. Aerosol impacts on cloud thermodynamic phase change over East Asia observed with CALIPSO and CloudSat measurements. J. Geophys. Res. Atmos. 120, 1490–1501. http://dx.doi.org/10.1002/2014JD022630.

Zhang, H., Wang, Z., Guo, P., Wang, Z., 2009. A modeling study of the effects of direct radiative forcing due to carbonaceous aerosol on the climate in East Asia. Adv. Atmos. Sci. 26 (1), 57–66. http://dx.doi.org/10.1007/s00376-009-0057-5.

Zhao, Y., Jiang, Y., Zhang, X., Lu, X., 2009. Research on the depoalrization ratio characteristic of the aerosol in the atmosphere with the CALIPSO satellite data. Acta Opt. Sinaca 29 (11), 2943–2951.

Zhou, L., Zhu, J., Zou, H., Ma, S., Li, P., Zhang, Y., Huo, C., 2013a. Atmospheric moisture distribution and transport over the Tibetan Plateau and the impacts of the South Asian summer monsoon. Acta Meteorol. Sin. 27 (6), 819–831. http://dx.doi.org/10.1007/s13351-013-0603-z.

Zhou, T., Huang, J., Huang, Z., Liu, J., Wang, W., Lin, L., 2013b. The depolarization-attenuated backscatter relationship for dust plumes. Opt. Express 21 (13), 15195–15204. http://dx.doi.org/10.1364/OE.21.015195.